

## Three-dimensional photovoltaics

Bryan Myers, Marco Bernardi, and Jeffrey C. Grossman

Citation: [Applied Physics Letters](#) **96**, 071902 (2010); doi: 10.1063/1.3308490

View online: <http://dx.doi.org/10.1063/1.3308490>

View Table of Contents: <http://scitation.aip.org/content/aip/journal/apl/96/7?ver=pdfcov>

Published by the [AIP Publishing](#)

---

### Articles you may be interested in

[Performance of smart maximum power point tracker under partial shading conditions of photovoltaic systems](#)  
J. Renewable Sustainable Energy **7**, 043141 (2015); 10.1063/1.4929665

[Two-dimensional plasmonic nanosurface for photovoltaics](#)  
J. Appl. Phys. **110**, 114313 (2011); 10.1063/1.3667194

[Will we exceed 50% efficiency in photovoltaics?](#)  
J. Appl. Phys. **110**, 031301 (2011); 10.1063/1.3600702

[Three-dimensional nanojunction device models for photovoltaics](#)  
Appl. Phys. Lett. **98**, 233106 (2011); 10.1063/1.3595411

[Semitransparent organic photovoltaic cells](#)  
Appl. Phys. Lett. **88**, 233502 (2006); 10.1063/1.2209176

---

The logo for AIP APL Photonics is displayed. It features the letters 'AIP' in a large, white, sans-serif font, followed by a vertical yellow bar and the words 'APL Photonics' in a smaller, white, sans-serif font. The background is a solid red color with a subtle, wavy pattern.

*APL Photonics* is pleased to announce  
**Benjamin Eggleton** as its Editor-in-Chief



## Three-dimensional photovoltaics

Bryan Myers,<sup>1</sup> Marco Bernardi,<sup>2</sup> and Jeffrey C. Grossman<sup>2,a)</sup>

<sup>1</sup>Department of Physics, University of California–Berkeley, Berkeley, California 94720, USA

<sup>2</sup>Department of Materials Science and Engineering, Massachusetts Institute of Technology, 77 Massachusetts Avenue, Cambridge, Massachusetts 02139-4307, USA

(Received 15 November 2009; accepted 11 January 2010; published online 16 February 2010)

The concept of three-dimensional (3D) photovoltaics is explored computationally using a genetic algorithm to optimize the energy production in a day for arbitrarily shaped 3D solar cells confined to a given area footprint and total volume. Our simulations demonstrate that the performance of 3D photovoltaic structures scales linearly with height, leading to volumetric energy conversion, and provides power fairly evenly throughout the day. Furthermore, we show that optimal 3D structures are not simple box-like shapes, and that design attributes such as reflectivity could be optimized using three-dimensionality. © 2010 American Institute of Physics. [doi:10.1063/1.3308490]

Significant efforts in materials selection and optimization of solar cell designs has led to three generations of photovoltaic (PV) architectures,<sup>1–6</sup> in which organic and inorganic materials are arranged to maximize exciton generation, and charge separation, transport, and collection based on the known physical processes taking place in the device.<sup>7</sup> Within this design space, the use of three-dimensionality has been confined to the nanostructuring of high-efficiency active layers<sup>8</sup> or to the micron scale arrangement of stacked layers in the cell. The pursuit of cost reduction well below the threshold of 1 \$/W<sup>5,6</sup> leaves no room for materials waste in most cases of technological interest. As a clear consequence, the planar arrangement of increasingly thin flat panels<sup>9</sup> has always been adopted to optimize the generated power-to-material ratio and avoid intercell shading. The flat panel shape also facilitates straightforward rooftop installation and is well suited to standard large-scale semiconductor fabrication techniques. The paradigm of the flat, quasi-two-dimensional solar cell has rarely been challenged.

Nevertheless, there are some practical situations and scenarios in which deviation from this scheme to include three-dimensionality on a macroscopic scale could prove relevant. A three-dimensional photovoltaic (3DPV) structure can absorb more light and generate more power than a flat panel of the same area footprint, which could prove useful in circumstances where the available area is limited. In addition, the introduction of three-dimensionality in PV could enable alternative fabrication routes, such as those based on 3D self-assembly of cheap and foldable substrates,<sup>10</sup> and may have the potential to lower installation costs. If we succeed in realizing a future of efficient and much less expensive PV materials,<sup>11</sup> then the shape and spatial arrangement of the solar cells may be among the key remaining variables to optimize. For these reasons, it is interesting to address a simple question; what would the optimal shape of a solar cell be, if it were 3D? Naively, a reasonable 3DPV shape would appear to be a box open at the top made of double-sided solar cells, as this arrangement (here referred to as “open-box”) intuitively allows for light trapping by multiple reflections. However, the answer is not so straightforward, as light reflection, incident angle, position with respect to the sun,

panel arrangement, and other factors define a complicated optimization problem.

In this letter, optimal 3DPV shapes are explored systematically using a combination of a genetic algorithm<sup>12,13</sup> (GA) and a code we developed to compute the energy generated in one day by an arbitrary shaped 3D solar cell. The solar-power-collecting structures are defined as configurations of triangles in Cartesian space confined to a rectangular box volume whose face normals point North, South, East, and West. The triangles represent double-sided flat panel solar cells, and within the GA are allowed to evolve their coordinates independently to produce an optimized 3D structure. In the GA, candidate 3D structures are combined using operations based on three principles of natural selection, namely, selection, recombination, and mutation. Selection determines which structures will propagate to the next step, where they are modified by the recombination and mutation operators.

The “tournament without replacement” selection scheme<sup>14</sup> was used, in which  $s$  structures from the current population are chosen randomly and the one with the highest value of a fitness function proceeds to the mating pool, until a desired pool size is reached. In our simulations  $s=2$ , and the fitness function corresponds to the energy that the individual structure produces in one day. Maximization of this energy is the single objective of our GA. The recombination step<sup>15</sup> randomly pairs 3D structures in the mating pool and with some probability (here 80%) crosses their triangle coordinates, causing the swapping of whole triangles. Finally, the mutation operator slightly perturbs each coordinate, for the purpose of searching more efficiently in coordinate space. These three operations are performed until convergence is reached, and a 3DPV structure with maximal energy production is achieved. A solar position algorithm<sup>16</sup> returned the azimuth and zenith angles of the apparent sun position as seen from the simulation location at successive time steps from sunrise to sunset (a time step of 12 minutes led to well-converged results). At each step, the simulation computed the total power incident on each triangle using ray-tracing to account for intercell shadowing and for the angle of incidence of the incoming light.<sup>17</sup> The number of triangles and the power conversion efficiency  $\eta$  were kept fixed during a single simulation. The spectral-averaged power reflectance  $R$  was given as a function of incident angle.<sup>18</sup> A total of 64 triangles were used in all cases, with reflectance  $R$

<sup>a)</sup>Electronic mail: jcg@mit.edu.

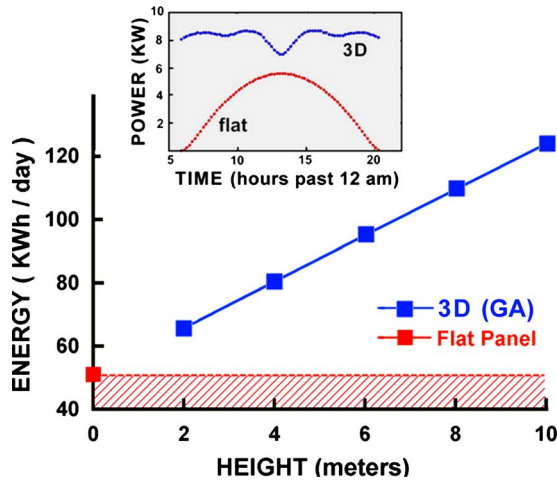


FIG. 1. (Color online) Plot of the energy produced in a day by GA-optimized 3DPV structures compared to that of a flat panel in the same conditions. The inset shows the power generated during the day for the flat panel compared to the 3DPV at height=10 m.

=4.1% at normal incidence and efficiency  $\eta=6\%$ .<sup>19</sup> Tests with a larger number of triangles (up to 1000) in the bounding volume did not show significant variation in the optimal 3D shape or energy produced. Energy values for 3D structures are lower bounds since we only implemented a single reflection per ray (to limit computation time) and did not account for ground reflections.

We optimized structures with a bounding-volume of area footprint (base area)  $10 \times 10 \text{ m}^2$  and height ranging from 2 to 10 m. Figure 1 shows the energy generated in a day as a function of the height of the GA-optimized 3DPV solar cell, compared to that of a flat panel of the same area footprint. The energy generated by the 3D structures scales linearly with height, thus leading to “volumetric” energy conversion. In addition, the power generated as a function of time during the day (inset, Fig. 1) shows a much more even distribution for 3DPV, due to the availability of cells with different orientations within the structure. The increase in power with height is dominant in the early morning and late afternoon, as expected, although the enhancement is broad in time and remains significant at all times during the day, even at mid-day. This even supply of power throughout the day can be “built-in” to a 3D structure, in contrast to power generated by a flat panel, which, without dual-axis tracking, decays rapidly around peak-time.

Interestingly, all the GA structures show similar patterns in their shapes, even for different heights. They contain no holes running across the bounding volume, which is necessary to intercept most of the incoming sunlight, and (less intuitively) they all have triangles coinciding with the 12 edges of the bounding box volume, so that they would cast the same shadow on the ground as the open-box. We emphasize that these patterns emerge from *randomly* generated structures, are not artifacts of the simulations, and are a fingerprint of emergent behavior resulting from the GA calculations.<sup>20</sup> The primary shape of the GA structure [Fig. 2(a)] is a box with its five visible faces caved in toward the midpoint. A simplified, symmetric version of this was constructed, as shown in Fig. 2(b); this idealized structure, which we refer to as the “funnel,” generates only 0.03% less energy in the day than the original GA output, and therefore

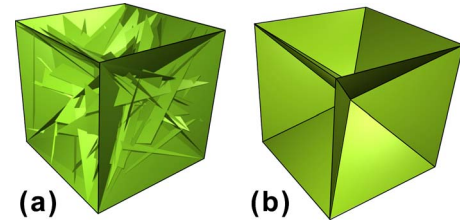


FIG. 2. (Color online) Schematics of 3DPV structures: (a) GA-optimized structure shown with all 64 triangles inside the bounding box; (b) funnel, a simplified version of most GA-optimized structures that retains their superior performance over other shapes.

contains most key ingredients of the complicated GA structures.

We compared the energy generated by simple open-box shapes and the funnel structures through a figure of merit  $M$ , defined as the ratio of the energy produced in a day to the total area of active material used, and scaled to one for the flat panel case. As can be seen in Table I, the energy of the funnel shape outperforms the open-box at all heights, and while both structures generate more energy than the flat panel case, they use excess material for a given energy (i.e.,  $M < 1$ ). For example, for a height of 10 m the open-box shape generates approximately  $2.38 \times$  as much energy as the flat panel but requires  $9 \times$  as much active material ( $M = 0.26$ ). The figure of merit for the open box decreases with height indicating that such a shape is not ideal for 3DPV in terms of efficient materials’ use. On the other hand, the GA-derived funnel shapes maintain a nearly constant figure of merit over this height range, with a cross-over to superior materials performance compared to the open-box at a height of  $\sim 5 \text{ m}$ , and 30% higher  $M$  at 10 m.

Despite the relatively small increase in energy generation of the GA shapes compared to the open box, these structures shed light on some fascinating aspects of 3DPV and may give significant practical advantages. The increase in produced energy of the best-performing GA structures is due to a decrease in the total power reflected to the environment and an increase in power generated using light reflected from other cells. This is easily seen by first disallowing the absorption of reflected rays, which results in a loss of roughly half of the increase in energy production. The remaining difference is eliminated if reflections are completely disabled (case  $R=0$ ), in which case the open-box and GA structures generate the same energy to within 0.005% agreement.

We also investigated how significant changes in reflectance might alter the optimal results. A 3D architecture could in principle be optimized to capture light using multiple reflections while preventing shading of the active material, possibly limiting the need for expensive antireflective

TABLE I. Energy produced in a day ( $E_{\text{box}}$  and  $E_{\text{funnel}}$ ) relative to the flat panel ( $E_0$ ) for the 3D open box and funnel structures, and corresponding figures of merit ( $M_{\text{box}}$  and  $M_{\text{funnel}}$ ) for an area footprint of  $10 \times 10 \text{ m}^2$ .

Height	$E_{\text{Box}}/E_0$	$E_{\text{Funnel}}/E_0$	$M_{\text{Box}}$	$M_{\text{Funnel}}$
2	1.29	1.29	0.49	0.36
4	1.56	1.58	0.37	0.36
6	1.83	1.87	0.32	0.36
8	2.11	2.15	0.29	0.35
10	2.38	2.43	0.26	0.34



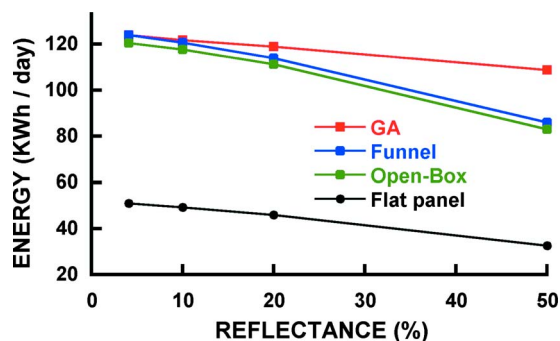


FIG. 3. (Color online) Energy produced in a day by PV structures made with materials of different reflectance, here defined as the ratio of the reflected power with the total incident power under solar illumination at normal incidence. The single-reflection approximation used here underestimates the energy produced at higher reflectance, so that the GA curve would have a smaller slope if the simulation accounted for infinite reflections.

coatings.<sup>2</sup> Such approaches based on intercell reflections are already a technological reality.<sup>21</sup> We varied the reflectance in the simulations using  $R=4.1\%$ ,  $10\%$ ,  $20\%$ , and  $50\%$  for a fixed volume of  $10 \times 10 \times 10 \text{ m}^3$  for all the shapes considered above, and performed separate GA optimizations for each value of  $R$ . Figure 3 shows that the performance decreases linearly in all cases for increasing reflectivity but with a much slower rate for the GA optimized structures than in all other cases. These trends indicate that for 3D solar cells it is possible to optimize the shapes such that materials within a relatively wide reflectance range can be used without significant deterioration of their performance, in contrast with current flat panel technology, deriving from intricate intercell coupling through reflection and reabsorption in 3DPV.

In summary, we have shown that 3DPV structures could provide substantially more energy in a day than flat panels of the same area footprint, and that shapes optimized using a GA approach may allow for significant materials saving and also the use of materials within a wide reflectance range without degradation of the device performance. The realization of such designs involves challenging practical aspects beyond materials selection, such as the assembly of the 3DPV architectures and the creation of 3D electrical connections and corresponding power electronics. Nonetheless, these results suggest that three-dimensionality presents interesting opportunities in PV design and solar energy generation.

This work was supported in part by NSF through the Network for Computational Nanotechnology, Grant No.

EEC-0634750. We are grateful to Professor Vladimir Bulovic for helpful discussions.

- <sup>1</sup>D. Ginley, M. A. Green, and R. Collins, *MRS Bull.* **33**, 355 (2008).
- <sup>2</sup>R. W. Miles, G. Zoppi, and I. Forbes, *Mater. Today* **10**, 20 (2007).
- <sup>3</sup>A. C. Mayer, S. R. Scully, B. E. Hardin, M. W. Rowell, and M. D. McGehee, *Mater. Today* **10**, 28 (2007).
- <sup>4</sup>M. A. Green, *Third Generation Photovoltaics: Advanced Solar Energy Conversion* (Springer, Berlin, 2005).
- <sup>5</sup>G. Conibeer, *Mater. Today* **10**, 42 (2007).
- <sup>6</sup>V. S. Arunachalam and E. L. Fleischer, *MRS Bull.* **33**, 264 (2008).
- <sup>7</sup>J. Nelson, *The Physics of Solar Cells* (Imperial College Press, London, 2003).
- <sup>8</sup>S. H. Park, S. Roy, S. Beaupré, S. Cho, N. Coates, J. S. Moon, D. Moses, M. Leclerc, K. Lee, and A. J. Heeger, *Nat. Photonics* **3**, 297 (2009).
- <sup>9</sup>R. M. Swanson, *Prog. Photovoltaics* **14**, 443 (2006).
- <sup>10</sup>D. H. Gracias, J. Tien, T. L. Breen, C. Hsu, and G. M. Whitesides, *Science* **289**, 1170 (2000); M. Boncheva, S. A. Andreev, L. Mahadevan, A. Winkelman, D. R. Reichman, M. G. Prentiss, S. Whitesides, and G. M. Whitesides, *Proc. Natl. Acad. Sci. U.S.A.* **102**, 3924 (2005).
- <sup>11</sup>V. Fthenakis, *Renewable Sustainable Energy Rev.* **13**, 2746 (2009).
- <sup>12</sup>For an introduction to the genetic algorithm approach, see D. E. Goldberg, *Genetic Algorithms in Search, Optimization, and Machine Learning* (Addison-Wesley Professional, Boston, 1989).
- <sup>13</sup>S. Kumara Illinois Genetic Algorithms Laboratory Report No. 2007016, 2007 (unpublished).
- <sup>14</sup>B. L. Miller and D. E. Goldberg, *Evol. Comput.* **4**, 113 (1996).
- <sup>15</sup>A two-point crossover recombination method was employed, wherein two indices are selected at random in the list of coordinates composing the chromosomes, and then the entire string of coordinates in between is traded between the pair of solutions.
- <sup>16</sup>I. Reda and A. Andreas, *Sol. Energy* **76**, 577 (2004). (We used the sun trajectory on a summer day in San Francisco for these particular calculations.)
- <sup>17</sup>The sun was assumed to be a source of parallel rays, and cloud-cover and all light-obstructions (except from other triangles in the structure) were neglected. For simplicity, it is assumed that all transmitted radiation counts toward the generated power, and only one reflection step (from solar cell surfaces) is taken into account. The triangles surfaces were assumed flat in the sense that all reflections were taken to be specular ( $\theta_{\text{refl}} = \theta_{\text{incid}}$ ); the opposite extreme, not implemented, would be Lambertian reflection, in which incident radiation scatters isotropically in the hemisphere. The number of ray-traces per cell (i.e., per triangle) was fixed to 100 during most simulations to limit computation time. After optimization, the final reported power values of the structures were evaluated with a larger standard number of ray-traces per cell (10 000), allowing convergence of the calculated energy value to better than 0.01%.
- <sup>18</sup>In the present work  $p$ -polarized light was assumed in the calculations. Extensive studies with unpolarized light are underway and will be discussed separately. Preliminary results suggest that the conclusions are consistent with this study, although unpolarized light leads to increased values of  $M$  due to the poorer performance of the flat panel.
- <sup>19</sup>We chose a typical for the average index of refraction (1.505) for organic active layers that would give  $R \sim 4\%$ . The efficiency was set to 6% to simulate the best performance of state-of-the-art polymer solar cells Ref. 8.
- <sup>20</sup>M. Mitchell, *Complexity: A Guided Tour* (Oxford University Press, New York, 2009).
- <sup>21</sup>See for example, P. R. Sharps, U.S. Patent Application No. 20090223554 (2009).